arXiv:1302.1709v1 [cond-mat.mes-hall] 7 Feb 2013

Theoretical analysis of spin qubit decoherence near optimal working points

S. J. Balian[1] and T. S. Monteiro[1]
[1]*Department of Physics and Astronomy, University College London,*
Gower Street, London WC1E 6BT, United Kingdom

(Dated: February 8, 2013)

We investigate suppression of various decoherence mechanisms at critical points variously termed optimal working points (OWPs) or clock transitions (CTs) of electron paramagnetic resonance (EPR) transitions in Si-based spin qubits, where the frequency – field gradient is zero ($df/dB = 0$). New experiments by Wolfowicz *et al.* [arXiv:1301.6567 (2013)] have demonstrated suppression of both instantaneous diffusion, as well as spin diffusion at these points, yielding orders of magnitude enhancement in coherence times: up to seconds, without extrapolation to zero-duration pulses as was until now necessary. We obtain simple analytical expressions and compare with full numerics, explaining the form of decoherence suppression for bismuth donors in Si (Si:Bi). It is demonstrated that behavior at the OWPs cannot be fully analyzed in terms of the behavior of df/dB, especially in the case of spin diffusion, indicating the need for an understanding at the level of the underlying microscopic processes entangling the central spin system and the spin bath.

PACS numbers: 76.30.–v, 76.60.Lz, 03.65.Yz, 03.67.Lx

I. INTRODUCTION

Coupled electronic-nuclear qubits have occupied a prominent role in the quest for robust and scalable quantum computing ever since the seminal proposal of Kane[1] for exploiting the long-lived coherence of nuclear qubits, in conjunction with the possibility for fast manipulation of the electron spin. Most work has considered phosphorus (^{31}P) donors in Si (Si:P).[1–12] In recent years, there has been growing interest in ^{209}Bi, the deepest Group V donor in Si (Si:Bi).[13–21] Various approaches for controlling decoherence have attracted considerable effort: dynamical decoupling techniques;[22–29] the use of so-called "clock transitions" (points at which the frequency–magnetic field gradient df/dB vanishes) in systems as diverse as flux qubits,[30] nuclear spin qubits[31–33] and electronic spin qubits of Si:Bi;[17,20] finally, studies of isotopically pure samples have indicated that electronic T_2 coherence times can be of order of seconds[34] while for nuclear spin qubits T_2 can reach minutes.[35]

Isotopic purification is effective in reducing decoherence because for donors in Si and other related systems, decoherence is primarily due to host impurities – ^{29}Si in the case of Si, since the ^{29}Si isotope (with natural abundance $p = 4.67$ %) has nuclear spin $I = 1/2$ and introduces spin diffusion, mainly by spin flip-flops. The availability of samples comprising almost pure ^{28}Si (which has no spin) might appear to offer a definitive solution by eliminating the decohering ^{29}Si spin-bath entirely. However, the previous measurements of intrinsic electronic T_2 times of order seconds in purified samples were extrapolated from the use of electron paramagnetic resonance (EPR) pulses of zero duration, in order to suppress instantaneous diffusion, a result of donor-donor interactions which otherwise limits T_2 to tens of milliseconds. Unfortunately, pulses of zero duration preclude a reasonable implementation of qubit rotations (e.g. a Hahn echo sequence) and restrict the possibilities for pulse sequences relevant to quantum information processing.

Now, a new experimental study of Si:Bi at CTs[36] demonstrated coherence times on macroscopic timescales without having to perform partial rotations and even for full-duration π-pulses. In addition, in natural Si, a factor of 100 enhancement in T_2 was observed at an OWP, to about 93 milliseconds. It has been previously demonstrated for Si:P that ^{29}Si nuclei suppress donor-donor flip-flops.[37] As pointed out in[36], the optimal situation might arise from a *combination* of partial enrichment and CTs.

Although CTs or optimal working points (OWPs) are of increasing interest, understanding of the underlying physics for spin decoherence is still lacking. Theoretical analysis is usually framed in terms of the qubit's reduced sensitivity to externally induced and uncorrelated magnetic field noise at the $df/dB = 0$ points; the T_2 behavior is then related to the curvature of the $f(B)$ function[31–33] including higher order behavior such as d^2f/dB^2. In previous studies using nuclear spin qubits,[31–33] these points are termed ZeFOZ (Zero First Order Zeeman Shift) points, rather than CTs, while in the earliest studies on flux qubits,[30] the term OWPs is used. For convenience, we refer to them as OWPs.

Parallel to these studies, the cluster correlation expansion (CCE) has provided a versatile and powerful framework for realistic simulation of the decoherence of a central spin in a spin bath.[37–47]. For the important problem of spin diffusion, the key physics leading to decoherence is entanglement between the bath and central spins.[43,44] Thus, analysis of decoherence in terms of sensitivity to a randomly fluctuating external magnetic field is at best an emergent behavior. We show in Fig. 1 by comparison with full CCE numerics, that the suppression of spin diffusion due to indirect flip-flops by bath spins cannot be described by df/dB, except locally.

In the present work, we obtain simple analytical expressions which clarify the physics of OWPs and explain the main experimental features. They are derived from a simplification of the CCE formalism (which we term "uCCE" for unperturbed CCE) using small clusters.

The analysis suggests that spin diffusion at OWPs is dominated by a relatively small proportion of strongly coupled spin clusters (i.e. for which the coupling to the central spin system is much stronger than the intrabath dipolar

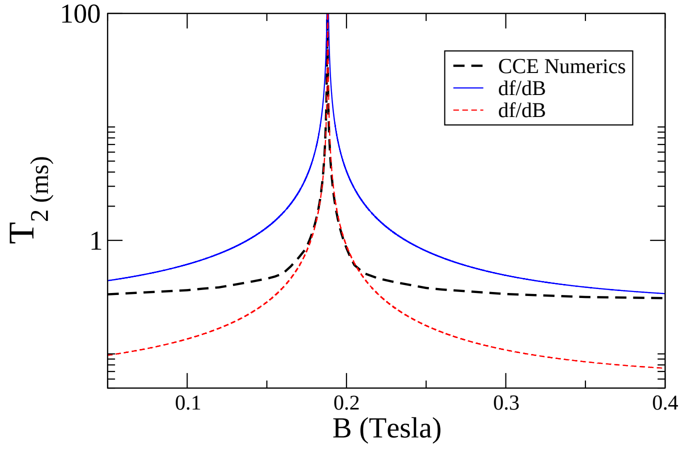

FIG. 1: (color online) Comparison between numerical T_2 times due to spin diffusion, calculated using the cluster correlation expansion and from df/dB. It can be seen that the behavior around optimal working points (OWPs) cannot be described by df/dB, except locally: the df/dB curve can either be scaled to agree with the asymptotic behavior (blue) or the inner region of the OWP (red) but not both. Thus, analysis of the underlying microscopic processes is essential to yield the full magnetic field dependence of $T_2(B)$.

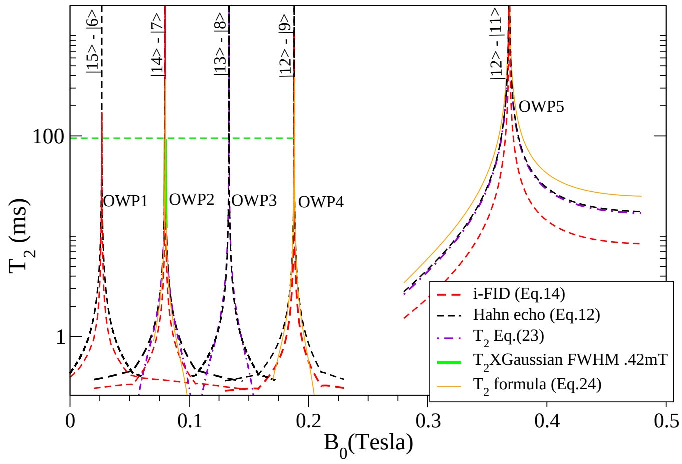

FIG. 2: (color online) Electron spin coherence times T_2, due to spin diffusion, at five Si:Bi EPR optimal working points (OWPs) evaluated for a Hahn echo sequence, FID and with our analytical formulae. Note that the analytical formula reproduces accurately the different shape of OWPs 1-4 relative to OWP 5. The latter is an NMR transition at high magnetic fields, but is an EPR transition at the OWP 5 point of $B = 0.37$ T. The green line indicates the result of convolving the behavior with a Gaussian of FWHM 2.1 G to allow for inhomogeneous broadening in natural Si. This reduces the maximum T_2 to about 100 ms. The intrinsic T_2 maximum for a single bismuth in natural Si at OWPs 1-4 is of order seconds, but experiments sample an ensemble of bismuth donors, with a 0.42 mT spread in field.

coupling between the flip-flopping bath nuclei). We obtain the shape of the OWP "spikes" ($T_2(B)$ plots) which for a single central spin system in a bath are limited to a maximum $T_2 \sim 10$ s. However, the upper limit to T_2 at OWPs for an ensemble of donors is of order 100 ms,[36] which here we attribute to inhomogeneous broadening. The uCCE expressions make clear the nature of the observed strong suppression of instantaneous diffusion and other donor-donor processes at OWPs in Ref. 36. We conclude that while the $T_2(B)$ due to indirect flip-flopping cannot be well described over the full range by a simple df/dB curve, in contrast, instantaneous diffusion, which is related to a simple energy shift, does follow an approximate $(df/dB)^2$ behavior, as seen experimentally.[21,36] This study does not eliminate the need for careful, high-order, large-cluster CCE numerics, which yield highly accurate quantitative results.[48] However, a key feature of the CTs is that the $T_2(B)$ curves can vary by over three orders of magnitude over an extremely narrow magnetic field range (tens of G) as seen in Fig. 2. Thus, we aim primarily to understand the underlying microscopic processes and to estimate $T_2(B)$ to within a factor of 2 or so.

This paper is organized as follows. In Section II, we develop a model of spin decoherence derived from the CCE and use it to obtain analytical expressions describing the behavior of OWPs. We apply the theory to nuclear spin diffusion in a bath of spin-1/2 nuclei, and further consider Si:Bi as the central spin system. In Section III, we present an analysis of donor-donor decoherence processes.

II. MICROSCOPIC THEORY OF NUCLEAR SPIN DIFFUSION AT OPTIMAL WORKING POINTS

A. Cluster correlation expansion

The methodology of the CCE is extensively detailed elsewhere both for a single central spin,[43,44] as well as an ensemble.[45] In calculating successive terms in the expansion, the Hamiltonian including a central spin system is diagonalized for sets or "clusters" of bath spins of varying sizes until convergence is achieved. The spin echo or free induction decay (FID) intensity computed for the largest cluster (containing the entire bath) as a function of time, t is denoted by $\mathcal{L}(t)$. It corresponds to the off-diagonal element of the central system's reduced density matrix, normalized to unity at $t = 0$. The expansion takes the form of

$$\mathcal{L}(t) = \prod_{\mathcal{K}} \tilde{\mathcal{L}}_{\mathcal{K}}(t). \quad (1)$$

where $\mathcal{K}$ denotes a cluster, and the product is over all clusters in the bath. Using Eq. (1), and defining $\mathcal{L}_{\mathcal{K}}(t)$ as the echo calculated for spins contained *only* in $\mathcal{K}$, a recursive expression for each cluster term ($\tilde{\mathcal{L}}_{\mathcal{K}}(t)$) is obtained:

$$\tilde{\mathcal{L}}_{\mathcal{K}}(t) = \mathcal{L}_{\mathcal{K}}(t) / \prod_{\mathcal{K}' \subset \mathcal{K}} \tilde{\mathcal{L}}_{\mathcal{K}'}(t). \quad (2)$$

The exact echo $\mathcal{L}(t)$ is recovered in the limit of including *all* clusters in the expansion. However, for spin diffusion, convergence is obtained by including only those clusters with at most a pair of bath spins. This is due to the large energy mismatch between the interaction among bath spins and the coupling of the central spin system to the bath.[41] A modified CCE was recently developed for the case when this energy mismatch is small.[48] More generally, the l-cluster CCE is defined as

$$\mathcal{L}^{(l)}(t) = \prod_{|\mathcal{K}|\leq l} \tilde{\mathcal{L}}_{\mathcal{K}}(t), \tag{3}$$

which includes clusters with at most l spins. We confirmed the expected convergence for spin diffusion as $l = 2 \rightarrow 3$.

B. Nuclear spin diffusion

Within the CCE framework, we consider a central spin system, which consists of an electron spin coupled to a nuclear spin, and interacting with a bath of other spins. The total Hamiltonian is written as

$$\hat{H}_{\text{tot}} = \hat{H}_0 + \hat{H}_{\text{int}} + \hat{H}_{\text{bath}}. \tag{4}$$

The first term denotes the Hamiltonian for the central spin system. In nuclear spin diffusion, the central spin system interacts with clusters of nuclear spins:

$$\hat{H}_{\text{int}} = \sum_n \hat{\mathbf{S}}\mathbf{J}_n\hat{\mathbf{I}}_n, \tag{5}$$

where $\mathbf{J}_n$ for the n-th spin is in general of tensor form (for anisotropic couplings). The final term represents the bath Hamiltonian including the Zeeman interaction with the external magnetic field B:

$$\hat{H}_{\text{bath}} = \sum_n \delta_N \omega_0 \hat{I}_n^z + \sum_{n<m} \hat{\mathbf{I}}_n \mathbf{D}(\mathbf{r}_{nm}) \hat{\mathbf{I}}_m, \tag{6}$$

where $\omega_0 = \mu B/\hbar$ is the electronic Larmor frequency ($\mu = 1.857 \times 10^{-23}$ JT^{-1}), δ_N is the ratio of the nuclear to electronic Larmor frequency and $\mathbf{r}_{nm}$ denotes the relative position vector of bath spins at lattice sites n and m. The components of the dipolar tensor $\mathbf{D}(\mathbf{r})$ are given by

$$D_{ij}(\mathbf{r}) = \frac{\mu_0 \delta_N^2 \mu^2}{4\pi\hbar r^3}\left(\delta_{ij} - \frac{3r_i r_j}{r^2}\right), \tag{7}$$

where δ_{ij} denotes the Kronecker delta, $\mu_0 = 4\pi \times 10^{-7}$ NA^{-2} and $i, j = x, y, z$.

C. uCCE approximation

While for the full CCE we would diagonalize $\hat{H}_{\text{tot}}$, here we introduce a simplified model. We first diagonalize $\hat{H}_0$:

$$\hat{H}_0 |i\rangle = E_0^{(i)} |i\rangle. \tag{8}$$

Typical values of $E_0^{(i)}$ are in the GHz range for electronic spin states. We then diagonalize $\hat{h}^{(i)} = \langle i| (\hat{H}_{\text{int}} + \hat{H}_{\text{bath}}) |i\rangle$, in other words the bath/interaction Hamiltonian averaged over the state of the central spin system. For nuclear spin diffusion, this is a reasonable approximation given $\hat{H}_0 \gg \hat{H}_{\text{int}}, \hat{H}_{\text{bath}}$ as the bath and interaction terms are on the kHz-MHz scale. Previous studies have employed the simplification of a bath evolution conditional on the state of the spin,[46,47] for systems where the central spin state is a simple electronic Zeeman state, whereas here we extend this to a more complex system comprising a highly mixed nuclear-electronic state, in the OWP regime. The key idea is still that the central spin regulates the bath evolution differently, depending on whether it is in the upper or lower states. However, here it is a strongly mixed state of ‘up’ and ‘down’ electronic/nuclear states, but the GHz scale of the central spin eigenfrequencies means that the bath ‘sees’ only the fast-averaged effective magnetic field. We proceed with diagonalizing the Hamiltonian $\hat{h}^{(i)}$ (and it is convenient here to use as a basis the states $|k_B\rangle$, which are eigenstates of the *non-interacting* bath). The eigenstates of $\hat{h}^{(i)}$ are:

$$\hat{h}^{(i)} |k_i\rangle = E_k^{(i)} |k_i\rangle \tag{9}$$

One immediate effect of the approximation is to in effect reduce the interaction with the bath to Ising form $\hat{H}_{\text{int}} \equiv J_n \hat{S}^z \hat{I}_n^z$ in Eq. (9). Since here we neglect coupling between the *nuclear spin* of the central spin system and the bath, in $\hat{h}^{(i)}$, we simply replace the operator $\hat{S}^z$ by the electronic polarization for each eigenstate (the difference between the probability for an up and a down electronic spin for the central spin system):

$$P_i(\omega_0) = 2\langle i| \hat{S}^z |i\rangle. \tag{10}$$

Near an OWP, $P_i(\omega_0)$ varies rapidly and by orders of magnitude with the external magnetic field B. For an unmixed state, $P_i(\omega_0) = \pm 1$. For an arbitrary $|u\rangle \rightarrow |l\rangle$ EPR transition, $|P_u - P_l| \simeq |df/dB|$. Nevertheless, it is worth noting that df/dB is a property of $\hat{H}_0$ (the central spin system) while P_u and P_l refer to the *interaction* term $\hat{h}^{(i)}$. As the former is of predominantly Ising form, dependence on P_u and P_l can *locally* be related to df/dB.

We now consider a Hahn echo sequence of an arbitrary $|u\rangle \rightarrow |l\rangle$ EPR transition. At time $t = 0$, the system is prepared by means of a $\frac{\pi}{2}$-pulse in the state $|t = 0\rangle$:

$$|t = 0\rangle = \tfrac{1}{\sqrt{2}}(|u\rangle + |l\rangle)|k_B\rangle, \tag{11}$$

the bath in initial state $|k_B\rangle$. A π-pulse is applied at $t = \tau$, then after further evolution for a second period τ, the corresponding Hahn echo for the $\mathcal{K}$-th spin cluster at $t = 2\tau$ is given by

$$\mathcal{L}^{u\rightarrow l}_{\text{Hahn}}(\mathcal{K}, k_B, t) = \sum_{k,k',j,j'=1,|\mathcal{K}|} \mathcal{C}^{u\rightarrow l}_{k,k',j,j'}(k_B)\, e^{-it\mathcal{E}^{u\rightarrow l}_{k,k',j,j'}}, \tag{12}$$

where

$$\begin{aligned} \mathcal{C}^{u\rightarrow l}_{k,k',j,j'}(k_B) &= \langle j'_u|j_l\rangle\langle k_u|j_l\rangle\langle j'_u|k'_l\rangle\langle k_u|k_B\rangle\langle k_B|k'_l\rangle, \\ \mathcal{E}^{u\rightarrow l}_{k,k',j,j'} &= E^l_j - E^u_{j'} + E^u_k - E^l_{k'}. \end{aligned} \tag{13}$$

Note that if we calculate $\sum_{k_B} \mathcal{L}^{u\rightarrow l}_{\text{Hahn}}(\mathcal{K}, k_B, t)$, we can use the completeness of the basis of non-interacting bath states to simplify Eq. (12). The intrinsic FID is simpler:

$$\mathcal{L}_{\mathrm{FID}}^{u\to l}\left(\mathcal{K},k_B,t\right)=\sum_{k,k'=1,|\mathcal{K}|}e^{-it\left(E_k^u-E_{k'}^l\right)} \\ \langle k_u|k_l'\rangle\langle j_u'|k_l'\rangle\langle k_l'|k_B\rangle\langle k_B|k_u\rangle \tag{14}$$

We note that the above expressions are valid for any cluster size, $|\mathcal{K}|$, not just two-clusters. The key assumption above (in addition to neglecting the non-Ising part of the interaction between the central spin system and the bath) is that since $\hat{H}_0 \gg \hat{H}_{\mathrm{bath}}$ we also neglect the "back-action" of $\hat{h}^{(i)}$ on the central spin states: $P_i\left(\omega_0\right)$ is evaluated without considering the interaction term. We refer to Equations (12) and (14) as uCCE ("unperturbed-state CCE") simply to distinguish them from the numerical results of the CCE arising from full diagonalization of $\hat{H}_{\mathrm{tot}}$. Below we investigate primarily two-cluster uCCE (i.e. $|\mathcal{K}|=2$) but test full numerics with $|\mathcal{K}|=3$. One advantage of the uCCE is the significant computational saving. For bismuth donors and similar systems in ^{29}Si baths, our comparisons suggest they are extraordinarily accurate to within 0.1 G of the OWP point. In general, they follow in detail the equivalent behavior obtained from full diagonalization which includes the non-Ising part of the system-bath interaction.

A potential advantage for an OWP investigation, is that the the $\mathcal{L}_{\mathrm{Hahn}}^{u\to l}\left(\mathcal{K},k_B,t\right)$ in Equations (12) and (14) typically oscillate on the kHz scale, while the comparable CCE quantity oscillates on the GHz scale. Near OWPs, we may wish to propagate $\mathcal{L}(t)$ on a millisecond timescale at one magnetic field, while at a nearby field we may need to propagate on the timescale of nearly a minute; i.e. while E_k^u and $E_{k'}^l$ are individually on GHz timescales, the $E_k^u-E_{k'}^l$ *differences* in Equations (12) and (14) are comparatively small. The elimination of this potential numerical problem may make propagation of the uCCE on macroscopic timescales more stable.

D. Spin diffusion from spin-1/2 flip-flops

In natural Si, the limiting decoherence mechanism at low temperatures is spin diffusion in a bath of spin-1/2 ^{29}Si impurities. Experimentally, decay of the Hahn echo for electronic spin qubit systems is typically fitted to $\exp[-t/T_2-(t/T_{\mathrm{SD}})^n]$, where $T_{\mathrm{SD}}<1$ ms characterizes the spin diffusion with $n\simeq 2$,[41] and other processes represented by T_2. Although $T_2 \gg T_{\mathrm{SD}}$, for convenience, we refer to our calculated decay time-scale as T_2 below, noting that we are in fact investigating spin diffusion.

Conveniently, Eq. (14) reduces to simple algebraic expressions: there is no need at all to undertake any numerical diagonalization in order to compute T_2. This suffices to reproduce most of the complexities of the Si:Bi OWP behavior described below.

For spin 1/2 systems like ^{29}Si, bath states $|k_B\rangle$ correspond to $|\uparrow\downarrow\rangle$, $|\downarrow\uparrow\rangle$, $|\uparrow\uparrow\rangle$ and $|\downarrow\downarrow\rangle$. We note that $|\uparrow\uparrow\rangle$ and $|\downarrow\downarrow\rangle$ cannot flip-flop, thus in our simple (Ising-only system-bath interaction) model, provide no decoherence. For the flip-flop states $|\uparrow\downarrow\rangle$ and $|\downarrow\uparrow\rangle$, we just diagonalize a simple 2×2 Hamiltonian analytically, obtained from

$$\hat{h}^{(u,l)}=(P_{u,l}\sum_{j=1,2}J_j\hat{I}_j^z)+C_{12}\left[\hat{I}_1^z\hat{I}_2^z-\tfrac{1}{4}\left(\hat{I}_1^+\hat{I}_2^-+\hat{I}_1^-\hat{I}_2^+\right)\right], \tag{15}$$

corresponding to a single cluster of two ^{29}Si spins interacting with dipolar coupling strength C_{12}, and each coupled to the central spin system with strength J_1 and J_2 respectively. Let i denote either u or l (ie the upper/lower states of the EPR transition). We introduce the parameters $\zeta_i^{\mathcal{K}}=(J_1^{\mathcal{K}}-J_2^{\mathcal{K}})P_i$ and $\epsilon_i=\sqrt{((C_{12}^{\mathcal{K}})^2+(\zeta_i^{\mathcal{K}})^2)}$. For simplicity, below we drop the cluster label $\mathcal{K}$, but it is understood that all quantities are calculated for a single ^{29}Si spin-pair, of which there are $N\sim 10^4$ in the bath. The eigenvalues are $4E_\pm^i=-C_{12}\pm\epsilon_i$. Defining $\xi_\pm^i=\zeta_i\pm\epsilon_i$, the eigenstates are

$$|i,\pm\rangle=a_i^\pm\,|\downarrow\uparrow\rangle\,|i\rangle+b_i^\pm\,|\uparrow\downarrow\rangle\,|i\rangle \tag{16}$$

with $a_i^\pm=C_{12}[(\xi_\pm^i)^2+C_{12}^2]^{-1/2}$ and $b_i^\pm=\xi_\pm^i[(\xi_\pm^i)^2+C_{12}^2]^{-1/2}$. The eigenstate overlaps (e.g. $\langle k_u|k_l'\rangle$) in Equations (14) and (12) are trivially evaluated from the $a_i^\pm$ and $b_i^\pm$. We thus rewrite:

$$2\mathcal{L}_{\mathrm{FID}}^{u\to l}(\mathcal{K},\uparrow\downarrow,t)=D_{ul}^+e^{-i(\epsilon_u-\epsilon_l)t}+D_{ul}^-e^{+i(\epsilon_u-\epsilon_l)t} \\ +R_{ul}^+e^{-i(\epsilon_u+\epsilon_l)t}+R_{ul}^-e^{+i(\epsilon_u+\epsilon_l)t} \tag{17}$$

where

$$D_{ul}^\pm=\frac{C_{12}^2((C_{12}^2+\xi_\pm^u\xi_\pm^l)}{\left[(C_{12}^2+(\xi_\pm^u)^2)(C_{12}^2+(\xi_\pm^l)^2)\right]}, \\ R_{ul}^\pm=\frac{C_{12}^2((C_{12}^2+\xi_\pm^u\xi_\mp^l)}{\left[(C_{12}^2+(\xi_\pm^u)^2)(C_{12}^2+(\xi_\mp^l)^2)\right]}. \tag{18}$$

The expression for $\mathcal{L}_{\mathrm{Hahn}}^{u\to l}(\mathcal{K},\uparrow\downarrow,t)$ is analogous, but much more complex. In addition, $\mathcal{L}_{\mathrm{FID}}^{u\to l}(\mathcal{K},\uparrow\uparrow,t)=\mathcal{L}_{\mathrm{FID}}^{u\to l}(\mathcal{K},\downarrow\downarrow,t)=1$. Thus we can replace the average over bath states by the simple approximation $\left\langle\mathcal{L}_{\mathrm{FID}}^{u\to l}\right\rangle\approx\frac{1}{2}+\frac{1}{2}\mathcal{L}_{\mathrm{FID}}^{u\to l}(\mathcal{K},\uparrow\downarrow,t)$.

The suppression of decoherence at OWPs is considerably clarified by Eq. (14). It gives the decay for a single cluster (the decay for the whole bath is $\mathcal{L}_{\mathrm{FID}}^{u\to l}(t)=\prod_{\mathcal{K}}\mathcal{L}_{\mathrm{FID}}^{u\to l}(\mathcal{K},t)$) and comprises four oscillating terms. At the OWP, $\epsilon_u=\epsilon_l$ so the terms dependent on $D^\pm$ cease to oscillate and stop contributing to decoherence. The $R^\pm$ terms continue to oscillate, rapidly. However, with some manipulation it is easy to show that at the OWPs, while $D^\pm\to 1$, the $R^\pm\to 0$, in other words, the amplitude of the rapidly oscillating terms vanishes. The decay behavior close to OWPs is entirely dominated by the $R^\pm$ terms.

E. Application to bismuth donors in Si

The Si:Bi system has an electron spin $S=1/2$ coupled to a large nuclear spin $I=9/2$ by a strong hyperfine coupling constant, $\frac{A}{2\pi}=1475.4$ MHz,

$$\hat{H}_0=\omega_0\left(\hat{S}_z+\delta_{\mathrm{Bi}}\hat{I}_z\right)+A\mathbf{I}.\mathbf{S}, \tag{19}$$

where $\delta_{\mathrm{Bi}} = 2.486 \times 10^{-4}$ is the ratio of the bismuth nuclear to electronic Zeeman frequencies. Measurements suggest isotropic couplings dominate the system-bath interaction.[20] The eigenstates $|i\rangle$ correspond to $i = 1, 2 \ldots 20$. The quantum numbers i are used to identify EPR transitions as shown in Fig. 2, thus OWP 2 corresponds to the experimentally investigated CT in Ref. 36 ($|14\rangle \to |7\rangle$ in the above notation).

The only parameter required to calculate a T_2 time, in addition to a set of coupling strengths C_{12}, J_1 and J_2, is the polarization P_i of the central spin eigenstates. The polarization is strongly field dependent near OWPs. The energy eigenstates $|i\rangle$ of Si:Bi near OWPs are strongly mixed and are not well approximated by the usual Zeeman basis $|m_S, m_I\rangle$. The mixed eigenstates may be labeled in an adiabatic basis and correspond to doublets of constant $m = m_S + m_I$:

$$|i\rangle = |\pm, m\rangle = \alpha_m^{\pm} \left|\pm\tfrac{1}{2}, m \mp \tfrac{1}{2}\right\rangle + \beta_m^{\pm} \left|\mp\tfrac{1}{2}, m \pm \tfrac{1}{2}\right\rangle . \quad (20)$$

All quantities are easily obtained analytically.[17] The electron polarization as a function of magnetic field is

$$P_i(\omega_0) = \Omega_m \left(\Omega_m^2 + 25 - m^2\right)^{-1/2} , \quad (21)$$

and $\Omega_m = m + \frac{\omega_0}{A}(1 + \delta_{\mathrm{Bi}})$; m is an integer $-5 \le m \le 5$. For the experimentally observed transition in Ref. 36, $m = -1$ for the upper state, while $m = -2$ for the lower state.

The simple expression Eq. (17) matches accurately to (within $\sim 1\%$ or so) the decay behavior of a corresponding numerical CCE calculation, whether far from OWPs or within the ~ 100 G width of OWPs 1-4. The only disagreement is well within 0.1 G of the OWP, where the full numerics suppress the divergence in T_2.

Figure 3 illustrate our results. We plot only uCCE FID results from Eq. (17) since the results from full CCE FID numerics were completely indistinguishable in the plots displayed. The only exception is the regime within 0.1 G of the OWP: the uCCE results yield $T_2 \to \infty$ at the actual OWPs, whereas the full numerics saturate at $T_2 \simeq 10$ s. This is beyond the range shown in our main result in Fig. 2. For natural Si, this discrepancy does not affect the measured results, since inhomogeneous broadening of 4.2 G means that the weight of the region within 0.1 G of the center is rather small.

Failure of convergence indicating the need for inclusion of higher-order corrections (larger clusters) manifests as oscillatory (non-decaying) behavior in our calculated Hahn echos as a function of time, at longer time scales. This does occur as we approach an OWP. A simple expedient (for a non-converged calculation) is to consider the decay rate at short times as it can provide a reasonable indication of the magnitude of T_2: inclusion of higher-order effects prolongs the calculation rather than radically changing T_2. However, fortunately, for reasonable parameters, the calculated FID does not fail and always displays non-oscillatory decay at all timescales. Thus, within about 50 G of the OWP, $T_{2-\mathrm{Hahn}}$ begins to fail; it ceases to decay at long times, and exhibits oscillations heralding loss of convergence. We can extend convergence times by using larger clusters, but cannot prolong this to the seconds timescales relevant to OWPs due to computational costs. In the experiment, the FID is affected by inhomogeneous broadening as it arises from an ensemble of bismuth donors, so the Hahn echo is essential. Our calculated FID in contrast is the intrinsic decay of a single bismuth donor. This intrinsic FID (termed iFID), away from OWPs, differs negligibly from the Hahn echo and provides a reasonable estimate of the decay timescale throughout. Away from OWPs, $T_{2-\mathrm{Hahn}}$ differs from $T_{2-\mathrm{iFID}}$ by less than 10% at all timescales and there are no convergence problems for either. In Fig. 2 we show $T_{2-\mathrm{Hahn}}$ values near OWPs obtained from the short time behavior of the Hahn echo, showing that $T_{2-\mathrm{Hahn}} \simeq 2T_{2-\mathrm{iFID}}$, to an excellent approximation at all the OWPs.

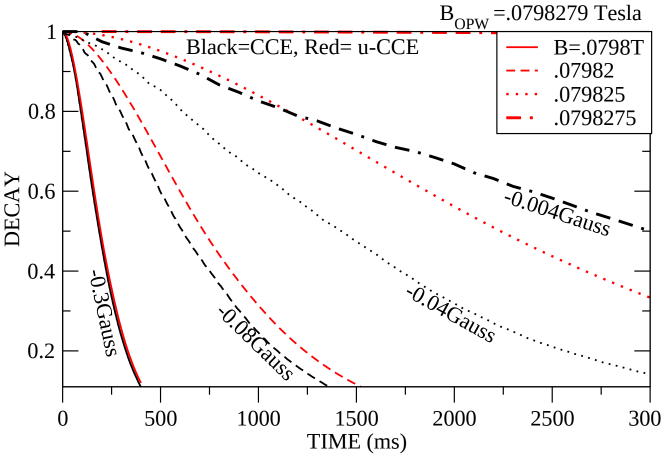

FIG. 3: (color online) Comparison between uCCE expressions (red) and CCE (black), showing excellent agreement up to within about 0.1 G of the OWP. We note that the width of the OWP 1-4 peaks is of order 100 G, as shown in Fig. 2, so uCCE fails over a very narrow region. Within about 0.01 G of the OWP, the uCCE T_2 time diverges while the CCE is limited to a maximum T_2 of order 10 s.

F. Approximate T_2 expressions near OWPs

We now derive analytical T_2 formulae, assuming $T_{2-\mathrm{Hahn}} \simeq 2T_{2-\mathrm{iFID}}$ represents a reasonable approximation to the decay timescale. From Eq. (17), from the short time behavior we can infer that *close to an OWP* each cluster $\mathcal{K}$ contributes $|\mathcal{L}^{u\to l}(\mathcal{K}, t)| \approx \exp\left[-(t/T_2^{\mathcal{K}})^2\right]$ where

$$\frac{1}{(T_2^{\mathcal{K}})^2} \approx \frac{10^6}{4}\left(R_{ul}^{+} + R_{ul}^{-}\right)(\epsilon_u + \epsilon_l)^2 \quad (22)$$

The above result is obtained by noting that near an OWP, $\epsilon_u \to \epsilon_l$ (easily shown) and $(D_{ul}^{+} + D_{ul}^{-}) \to 1$, while $R^{\pm} \to 0$. The total T_2 is obtained by summing over all clusters:

$$\frac{1}{T_2^2} = \sum_{\mathcal{K}=1}^{\mathcal{K}\simeq 10^4} \frac{1}{(T_2^{\mathcal{K}})^2} \quad (23)$$

Equation (23) predicts the intrinsic FID behavior. Doubling it represent an estimate of the Hahn echo decay. The above expression is displayed for OWPs 2, 3 and 5 in Fig. 2

showing excellent agreement (violet dot-dashed lines) very near the OWPs.

In Fig. 4 we use Eq. (23) to estimate the strength of the $\mathcal{K}$-th ^{29}Si spin pair's individual contribution to decoherence (its $1/(T_2^{\mathcal{K}})^2$) as function of the hyperfine coupling to the central spin. Note that J_1 and J_2 always appear as a difference in the equations, thus $|J_1 - J_2|$ is the relevant parameter. A striking pattern appears: the spins are grouped into lines of constant C_{12}, corresponding to adjacent spins, second nearest neighbor and so forth. Surprisingly, for the stronger spins, the $1/(T_2^{\mathcal{K}})^2$ is completely independent of the hyperfine coupling to the central spin. The origin of this behavior is clear from Eq. (22). For large $|J_1 - J_2| \gg C_{12}$, the amplitudes $R^+_{ul} + R^-_{ul} \propto \frac{1}{(J_1 - J_2)^2}$ while the frequency of the oscillation $(\epsilon_u + \epsilon_l)^2 \propto (J_1 - J_2)^2$, eliminating the dependence on the coupling. This conclusion must be approached with some caution. Eq. (22) is valid only near the OWP and refers to short time decay behavior. Nevertheless, numerical test s do indicate insensitivity to the hyperfine coupling in the strongly coupled spins. The pattern persists unchanged for nearby B values.

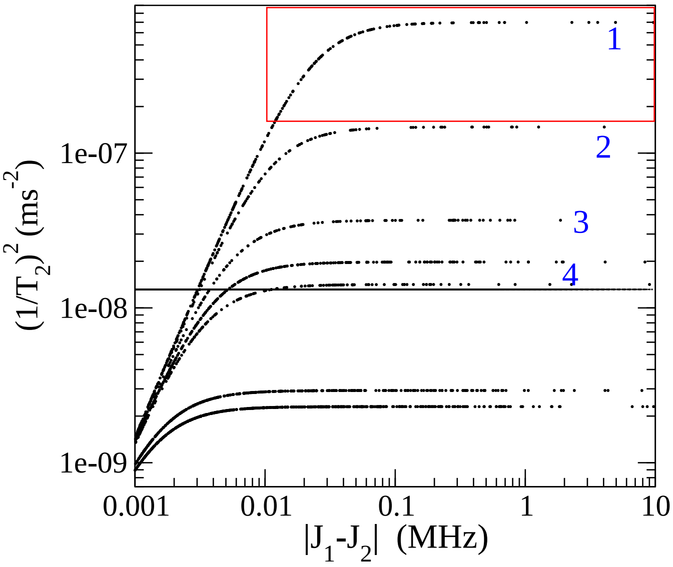

FIG. 4: Estimated weight of each spin in the bath (a total of 10^4 flip-flopping pairs, as indicated by their individual contribution the total $(1/T_2)^2$, plotted as a function of the strength of the hyperfine coupling to the central spin system. We see that the ^{29}Si spins in the bath fall neatly into groups corresponding to different C_{12}: here $n = 1, 2, 3..$ indicate nearest neighbors on the lattice, second-nearest and so forth. This behavior is valid only close (within $\simeq$ 100 G) of the OWPs. The scale of T_2 is set by the comparatively small $N \sim 10^2$ set of strongly-coupled spins in the red box. Data corresponds to $B = 0.07978$ T, i.e. about 0.5 G from the maximum of OWP 2.

What is striking is that in Fig. 2, the $N \sim 10^2$ strongest spin pairs suffice to set the scale of T_2. We have tested this by running a two-cluster CCE calculation with just 120 spins. The FID yield $T_2 \simeq 140$ ms with all $\sim 10^4$ spins and $T_2 \simeq 160$ ms with just these spins. All these spins correspond to $|J_1 - J_2| \gg C_{12}$ and also to the strongest values of nearest-neighbor dipolar coupling $C_{12} = 0.23 \times 10^{-2}$ MHz.

We can use this to derive an approximate formula for decoherence near OWPs:

$$T_2 \times 10^3 \approx \frac{16}{\overline{C}_{12}\sqrt{N}} \frac{\sqrt{|P_u(\omega_0) P_l(\omega_0)|}}{|P_u(\omega_0) - P_l(\omega_0)|}. \tag{24}$$

The 10^3 scaling simply ensures an answer in milliseconds as all our energy units are in MHz. From the above, we estimate $\overline{C}_{12}\sqrt{N} \simeq 0.024$ MHz. Over the narrow OWP 1-4, $\sqrt{|P_u(\omega_0) P_l(\omega_0)|}$ is nearly constant, thus the field dependence reduces to $1/(P_u - P_l)$. Since $(P_u - P_l) \propto df/dB$ there is an approximate $(df/dB)^{-1}$ dependence close to the OWP. However, the additional $\sqrt{|P_u(\omega_0) P_l(\omega_0)|}$ term in the numerator accounts for the much larger T_2 in OWP 5, without the need for scaling or fitting parameters, indicating that the $(df/dB)^{-1}$ does not represent the full field dependence.

From Eq. (24), we infer that the intrinsic T_2 depends on $1/\sqrt{p}$ where $p = 4.67$ % the percentage of ^{29}Si in natural Si. Given that the inhomogeneous line width also varies as $1/\sqrt{p}$, the combined dependence should be linear $\sim 1/p$. It is reasonable to assume that the T_2 limit of 100 ms in natural Si will reach the seconds timescale for very modest enrichment factors of 100. Above this level, donor-donor effects are the limiting factors.

All the uCCE expressions indicate a divergence at the OWP. However, this presupposes that all spin clusters can achieve the condition $P_u(\omega_0) = P_l(\omega_0)$ at the same external magnetic field ω_0. In reality, $H_{\rm bath}$ does very slightly perturb the H_0 eigenstates in Eq. (8). The hyperfine coupling to the bath provides a small correction to the former and by implication to the polarization, $P_u(\omega_0) \rightarrow P_u(\omega_0 + \delta B)$ where $\delta B \sim \left\langle \left(|a_i^k|^2 - |b_i^k|^2 \right) (J_1 - J_2)/4 \right\rangle$. In addition, there is a correction from the non-Ising part of the interaction, which mixes the bismuth eigenstates. Full CCE numerics diverges from uCCE within 0.1 G of the OWP. Within ~ 0.01 G the two-cluster CCE results indicate a maximum T_2 of 10 s, suppressing the divergence. This is the true limit for a singl central spin system in a bath. However there are other sources of spread in the effective external field due to the fact that the experiment samples an ensemble of bismuth donors, subject to variations in the local fields. One is the local variation in A, the bismuth hyperfine constant, due to lattice strain.[36] With a 200 kHz line width[21] this represents also a < 0.1 G spread. More drastic is the line width of natural Si, arising from the sea of single ^{29}Si spins (more numerous than the spin pairs responsible for spin diffusion) which cause a variation in B among spin qubits. This is of order 0.42 mT. Hence we convolve the OWP 2 behavior with a Gaussian to simulate this effect. We calculate the time decay

$$D(t) = \frac{1}{w\sqrt{2\pi}} \int e^{\frac{(B - B_{\rm OWP})^2}{2w^2}} e^{(t/T_2(B))^2} dB \tag{25}$$

where $w = 0.21$ mT and $T_2(B)$ is our calculated T_2 values. $D(t)$ is found to give a non-Gaussian decay (stretched exponential) as observed and reaches its e^{-1} value at 100 ms. Figure 2 also shows the result (green curve): the maximum T_2 attainable OWP 1-4 in natural Si is of order 100 ms.

The close agreement with the experimental value of 93 ms is fortuitous: our analysis aims only for accuracy of a factor of order 2 or so, but this gives an indication of the expected experimental behavior.

When using uCCE expressions rather than full numerics, we imposed a cut-off in the maximum $T_2 = 10$ s very close to the OWP and do not permit higher values. However, the convolution is not at all sensitive to the manner this intrinsic limit of 10 s from CCE numerics is imposed: the uCCE divergence is extremely narrow, thus the uCCE remains a reliable approach.

III. DONOR-DONOR DECOHERENCE

For the purest isotopically enriched samples, decoherence by ^{29}Si bath impurities is eliminated and the coherence times are instead limited by donor-donor spin interactions. The most destructive to previous experiments has been instantaneous diffusion. In a Hahn-like echo sequence, neighboring donor spins are also rotated by applied pulses: this is especially problematic for the second, π-pulse, as it leads to a temporally changing field whose effects are not removed by the echo sequence.[49,50] The other relevant processes are indirect flip-flops, whereby a central donor interacts with a bath of dipole-coupled donors, and direct flip-flops which involves the central donor flip-flopping with a bath donor. The latter is the limiting decoherence process.

A. Instantaneous diffusion

In this case, for uCCE, we revisit the key Hamiltonian in Eq. (26) which now has simply two donor spin systems, spins A and B (which can be hybrid electronic-nuclear states or more complex systems).

$$\hat{H}_{\text{tot}} = \hat{H}_0^A + \hat{H}_0^B + \hat{H}_{\text{int}} \tag{26}$$

where $\hat{H}_{\text{int}} = D_{\mathcal{K}} S_A^z S_A^z$ for coupling between donor-donor pair $\mathcal{K}$. We diagonalize H_0^A and H_0^B then consider the averaged interaction field $\langle i_A i_B | \hat{H}_{\text{int}} | i_A i_B \rangle$. We consider the pulse sequence

$$e^{-i\hat{H}\tau} - R_x^A\left(2\theta_A\right) R_x^B\left(2\theta_B\right) - e^{-i\hat{H}\tau}, \tag{27}$$

meaning that the central spin A experiences a rotation of tip-angle θ_A (which in a Hahn sequence is $2\theta_A = \pi$) while the 'bath' spin B, unintentionally flipped by the pulse, undergoes a rotation by tip-angle θ_B (which in general need not be identical to θ_A). Here, R_x represents a rotation about the x-axis of the Bloch sphere.

We assume the initial state to be $\frac{1}{\sqrt{2}}\left(|m\rangle + |n\rangle\right)_A |m\rangle_B$. Since both A and B have to be resonant with the pulse, their spin states must correspond to either of the states of the EPR transition i.e. $m, n \equiv u, l$ for $|u\rangle \to |l\rangle$. The echo is given by:

$$\begin{aligned} |\mathcal{L}\left(2\tau\right)| &= \tfrac{1}{2}\left| e^{i\tau\left(E_m - E_n - \frac{DP_m(P_n - P_m)}{4}\right)} \sin\theta_A + \cos\theta_A \right|^2 \\ &\quad \times \left| e^{\frac{i\tau D(P_m - P_n)^2}{4}} \sin^2\theta_B + \cos^2\theta_B \right|. \end{aligned} \tag{28}$$

where $D_k \equiv D$ for convenience. This equation is equivalent to Eq. (14), but requires little further analysis. By inspection, we see that at the OWP, where $P_n = P_m$, the echo is suppressed quadratically in $(P_m - P_n)$. The spin-bath coupling strength D vanishes from the expression and in the second term, the tip-angle of the bath spin θ_B also vanishes entirely, making the decay rate completely independent of the angle that the bath spin is (unintentionally) rotated through:

$$|\mathcal{L}\left(2\tau\right)|_{\text{OWP}} = \frac{1}{2}\left| e^{i\tau E_n}\cos\theta_A + e^{i\tau E_m}\sin\theta_A \right|^2. \tag{29}$$

For a π pulse, $2\theta_1 = \pi$ and $|\mathcal{L}\left(2\tau\right)|_{\text{OWP}} = 1$ for all B spins, regardless of coupling strength or θ_B.

B. Indirect flip-flops

The case of indirect flip-flops is analogous to a pair of flip-flopping ^{29}Si's with the hyperfine couplings to nuclei replaced by dipolar couplings to a pair of donor electrons. The couplings to the central donor are scaled by the polarizations P_m and P_n and the coupling between bath donors by $\left(\alpha_m\alpha_n\right)^2$. In addition, the eigenvalues of the interaction Hamiltonian are shifted by $+\frac{1}{4}c_{mn}\left(1 - P_m P_n\right)$. Like ^{29}Si spin diffusion, indirect flip-flops are suppressed linearly in $(P_m - P_n)$ at OWPs as discussed above.

C. Direct flip-flops

Direct flip-flops are not suppressed at OWPs and limit the electron T_2 at low temperatures. The effective Hamiltonian is $\hat{H} = \hat{H}_0^A + \hat{H}_0^B + \hat{H}_{\text{int}}$ with

$$\hat{H}_{\text{int}} = D\hat{S}_A^z\hat{S}_B^z + \tfrac{D}{4}\left(S_A^+ S_B^- + S_A^- S_B^+\right). \tag{30}$$

For the initial state $\frac{1}{\sqrt{2}}\left(|m\rangle + |n\rangle\right)_A |m\rangle_B$, the FID is given by

$$|\mathcal{L}\left(\tau\right)| = \left|\cos\left(\frac{\tau D\alpha_m^2\alpha_n^2}{4}\right)\right|, \tag{31}$$

and for a coherent superposition of $|m\rangle_B$ and $|n\rangle_B$ in the initial state,

$$|\mathcal{L}\left(\tau\right)| = \sqrt{\frac{1 + \cos\left\{\frac{\tau D}{4}\left[\left(P_m - P_n\right)^2 + 2\alpha_m^2\alpha_n^2\right]\right\}}{2}}. \tag{32}$$

At an OWP, the $(P_m - P_n)^2$ term vanishes, but this is insufficient to eliminate the oscillations in $\mathcal{L}\left(\tau\right)$ which cause decoherence. Thus, direct flip-flops are not suppressed at OWPs.

IV. CONCLUSIONS

We present a theoretical analysis of spin decoherence near OWPs, which clarifies which decohering processes are suppressed and which are not. The method is a simplification of the CCE approach, but applicable to general central spin systems which are not single spin-1/2 systems (which have no OWPs). An advantage of the approach is that the central spin system need only be diagonalized once, thus saving significant computational time. In addition, evolution for longer time periods is more numerically stable. Thus this simplification may find applications even in regimes without OWPs. Our expressions for T_2 times are in agreement with full numerical diagonalization (ie application of the usual CCE method, including non-secular terms).

In applying the theory to Si:Bi nuclear spin diffusion, we find that the behavior of T_2 does not follow the form of df/dB except locally. Finally, we present an analysis of donor-donor decoherence effects which are known to limit T_2 in isotopically pure samples. As demonstrated in recent experiments, we explain the suppression of instantaneous diffusion at OWPs and show that direct donor-donor flip-flops provide the limiting decoherence mechanism at low temperatures.

Acknowledgments We are extremely grateful to Gary Wolfowicz and John Morton for helpful suggestions and explanation of their experimental results. We also gratefully acknowledge discussions with Hamed Mohammady, Gavin Morley, Chris Kay and Wayne Witzel.

---

[1] B. E. Kane, Nature **393**, 133 (1998).

[2] S. R. Schofield, N. J. Curson, M. Y. Simmons *et al.*, Phys. Rev. Lett. **91**, 136104 (2003).

[3] Kai-Mei C. Fu, T. D. Ladd, C. Santori, and Y. Yamamoto, Phys. Rev. B **69**, 125306 (2004).

[4] G. W. Morley, D. R. McCamey, H. A. Seipel *et al.*, Phys. Rev. Lett. **101**, 207602 (2008).

[5] S. Simmons, R. M. Brown, H. Riemann *et al.*, Nature **470**, 69 (2011).

[6] A. Morello, J. J. Pla, F. A. Zwanenburg *et al.*, Nature **467**, 687 (2010).

[7] L. Dreher, F. Hoehne, M. Stutzmann and M. S. Brandt, Phys. Rev. Lett. **108**, 027602 (2012).

[8] M. Steger, T. Sekiguchi, A. Yang *et al.*, J. Appl. Phys. **109**, 102411 (2011).

[9] A. M. Stoneham, A. J. Fisher and P. T. Greenland, J. Phys.: Condens. Matter **15**, L447 (2003).

[10] P. T. Greenland, S. A. Lynch, A. F. G. van der Meer *et al.*, Nature **465**, 1057 (2010).

[11] M. Fuechsle, J. A. Miwa, S. Mahapatra *et al.*, Nature Nanotech. **7**, 242 (2012).

[12] A. M. Tyryshkin, S. A. Lyon, A. V. Astashkin, and A. M. Raitsimring, Phys. Rev. B **68**, 193207 (2003).

[13] T. Sekiguchi, M. Steger, K. Saeedi, M. Thewalt *et al.*, Phys. Rev. Lett. **104**, 137402 (2010).

[14] G. W. Morley, M. Warner, A. M. Stoneham *et al.*, Nature Materials **9**, 725-729 (2010).

[15] G. W. Morley *et al.*, Nature Materials **12**, 103107 (2013).

[16] R. E. George, W. Witzel, H. Riemann *et al.*, Phys. Rev. Lett. **105**, 067601 (2010).

[17] M. H. Mohammady, G. W. Morley, and T. S. Monteiro, Phys. Rev. Lett. **105**, 067602 (2010).

[18] M. H. Mohammady, G. W. Morley, A. Nazir, and T. S. Monteiro, Phys. Rev. B **85**, 094404 (2012).

[19] M. Belli, M. Fanciulli, and N. V. Abrosimov, Phys. Rev. B **83**, 235204 (2011).

[20] Balian,S.J., Kunze,M.B.A., Mohammady M.H., Phys. Rev. B **86**, 104428 (2012).

[21] Gary Wolfowicz *et al.* Phys. Rev. B 86, 245301 (2012).

[22] N. Bar-Gill, L. M. Pham, C. Belthangady *et al.*, Nat. Commun. **3**, 858 (2012).

[23] de Lange, G., Wang, Z. H., Rist, D., Dobrovitski, V. V. & Hanson, R. Science **330**, 6063 (2010).

[24] Naydenov, B *et al.* Phys. Rev. B **83**, 081201 (2011).

[25] Ryan, C. A., Hodges, J. S. & Cory, D. G., Phys. Rev. Lett. **105**, 200402,(2010).

[26] Almog, I. et al., J. Phys. B: Atomic, Mol Opt. Phys. 44, 154006 (2011).

[27] Bylander, J. et al., Nat. Phys. 7, 565570 (2011).

[28] lvarez, G. A. & Suter, D., Phys. Rev. Lett. 107, 230501 (2011).

[29] Du, J. et al., Nature 461, 12651268 (2009).

[30] D. Vion, A. Aassime, A. Cottet *et al.*, Science **296**, 886 (2002).

[31] E Fraval, M.J.Sellars and J.J.Longdell, Phys. Rev. Lett. 95, 030506 (2015).

[32] J.J.Longdell, A.L.Alexander and M.J. Sellars, Phys. Rev. B **85**, 032339 (2012).

[33] D.McAuslan, J.Bartholomew, M.sellars and J.Longdell, Phys. Rev. B **74**, 195101 (2006)

[34] A. M. Tyryshkin, S. Tojo, J. J. L. Morton, H. Riemann, N. V. Abrosimov *et al.*, Nature Materials **11**, 143 (2012).

[35] M. Steger *et al.*, Science **336**, 1280 (2012).

[36] Gary Wolfowicz, Alexei M. Tyryshkin, Richard E. George, Helge Riemann, Nikolai V. Abrosimov, Peter Becker, Hans-Joachim Pohl, Mike L. W. Thewalt, Stephen A. Lyon, John J. L. Morton, arXiv:1301.6567.

[37] W. M. Witzel, M. S. Carroll, A. Morello, L. Cywinski, and S. Das Sarma, Phys. Rev. Lett. **105**, 187602 (2010).

[38] E. Abe *et al.*, Phys. Rev. B **82**, 121201(R) (2010).

[39] G. de Lange, T. van der Sar, M. Blok *et al.*, Sci. Rep. **2**, 382 (2012).

[40] S. Takahashi, R. Hanson, J. van Tol, M. S. Sherwin, and D. D. Awschalom, Phys. Rev. Lett. **101**, 047601 (2008).

[41] W. M. Witzel and S. Das Sarma, Phys. Rev. B **74**, 035322 (2006).

[42] E. Abe, K. M. Itoh, J. Isoya, and S. Yamasaki, Phys. Rev. B **70**, 033204 (2004).

[43] W. Yang and R. B. Liu, Phys. Rev. B **78**, 085315 (2008);

[44] W. Yang and R. B. Liu, *ibid.* **78**, 129901(E) (2008);

[45] W. Yang and R. B. Liu, *ibid.* **79**, 115320 (2009).

[46] N. Zhao, S. W. Ho, and R. B. Liu, Phys. Rev. B **85**, 115303 (2012).

[47] J.R. Maze, J.M. Taylor and M.D.Lukin, Phys. Rev. B **78**, 094303 (2008).

[48] W. M. Witzel *et al.*, Phys. Rev. B **86**, 035452 (2012).

[49] KM Salikhov, S.A.Dzuba, A.M. Raitsimring, J.Mag.Res., **42**, 255 (1981).

[50] A. Schweiger and G. Jeschke, in *Principles of Pulse paramagnetic resonance* (Oxford University, New York, 2001).